Olfactory fear conditioning biases olfactory stem cell receptor fate

Clara W. Liff [1], Yasmine R. Ayman [1], Eliza C.B. Jaeger [1], Hudson S. Lee [1], Alexis Kim[1,2], Bianca Jones Marlin[1,2,3]*

[1] Mortimer B. Zuckerman Mind Brain and Behavior Institute, Department of Neuroscience, Columbia University, New York, NY, 10027 USA
[2] Department of Psychology, Columbia University, New York, NY, 10032 USA
[3] Department of Neuroscience, Columbia University, New York, NY, 10032 USA

*To Whom Correspondence Should Be Addressed:
Bianca Jones Marlin, Ph.D.
Department of Psychology
Department of Neuroscience
Mortimer B. Zuckerman Mind Brain and Behavior Institute
Columbia University
3227 Broadway, New York, NY 10027
bjm2174@columbia.edu

SUMMARY

The main olfactory epithelium initiates the process of odor encoding. Recent studies have demonstrated intergenerationally inherited changes in the olfactory system in response to fear conditioning, resulting in increases in olfactory receptor frequencies and altered responses to odors. We investigated changes in the morphology of the olfactory sensory epithelium in response to an aversive foot stimulus. Here, we achieve volumetric cellular resolution to demonstrate that olfactory fear conditioning increases the number of odor-encoding neurons in mice that experience shock-odor conditioning (F0), *as well as their offspring* (F1). We provide evidence that increases in F0 were due to biased stem cell receptor choice. Thus, we reveal dynamic regulation of the main olfactory epithelium receptor composition in response to olfactory fear conditioning, providing insight into the heritability of acquired phenotypes.

GRAPHICAL ABSTRACT

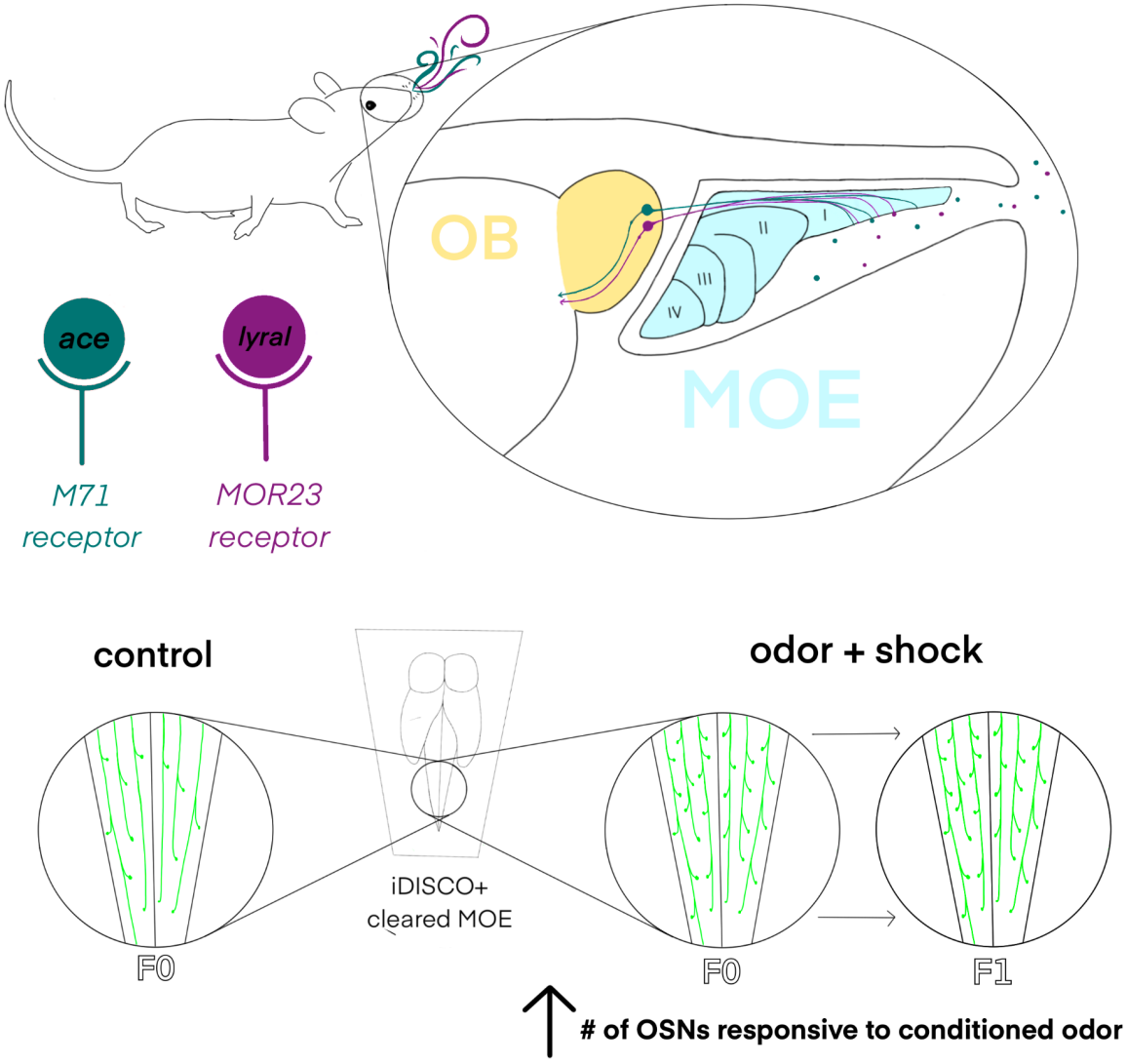

HIGHLIGHTS

- Olfactory fear conditioning leads to an increase in conditioned-odor-responsive cells in parents (F0) that is heritable (F1)
- Increase in conditioned-odor-responsive cells is sustained through at least 9 weeks of cell turnover in the main olfactory epithelium
- Olfactory fear conditioning in F0 biases neurogenesis specifically toward conditioned-odor-responsive cell fate

INTRODUCTION

Aversive olfactory conditioning in mice results in the persistent avoidance of the conditioned odor, and the olfactory sensory neurons (OSNs) responsive to this odor increase in number in the sensory epithelium (Jones et al., 2008). Strikingly, this increase in the number of specific sensory neurons was observed not only in trained F0 males, but also in their offspring (F1), despite the fact that the progeny had never been exposed to the conditioned odor (Dias & Ressler, 2014; Aoued et al., 2019; Aoued et al., 2020). This phenomenon, intergenerational epigenetic inheritance, invokes the transfer of information from one generation to the next without alterations to the sequence of the genome.

Transgenerational epigenetic inheritance, the transfer of information beyond the F1 generation, is responsible for several examples of non-Mendelian transmission in plants, fission yeast, and worms (Greer et al., 2011; Schmitz et al., 2011; Rechavi et al., 2014; Yu et al., 2018; Moore et al., 2021). Molecular genetics has provided a detailed mechanistic understanding of the transmission of epigenetic information from parent to offspring in these organisms (Rando & Verstrepen, 2007; Fitz-James & Cavalli, 2022). Olfactory conditioning in the parent may provide future generations with an adaptive advantage: enhanced sensitivity to aversive sensory features in the environment of the parent. Intergenerational epigenetic inheritance of olfactory properties in mice poses an elusive problem as to how signals responsible for the increase in specific OSNs in the sensory epithelium are transmitted from the nose, to the gamete, and then to the offspring.

Olfactory perception is initiated by the recognition of odorants by a large repertoire of receptors in the sensory epithelium. Individual sensory neurons in mice express only one of 1,400 different receptor genes (Buck & Axel, 1991). The choice of a receptor is stochastic and is mediated by an unusual mechanism of transactivation that delivers the necessary transcription factors to only one allele of a single receptor gene in a sensory neuron (Chess et al., 1994; Shykind et al., 2004; Lomvardas et al., 2006). Neurons expressing a given receptor are distributed within zones of the epithelium but project with precision to spatially invariant glomeruli in the olfactory bulb. Each odorant can interact with multiple distinct receptors, resulting in the activation of a unique ensemble of glomeruli. The recognition of an odor requires the integration of information from multiple glomeruli to the mitral and tufted cells in the olfactory bulb, and then to downstream olfactory convergent areas (Price & Powell, 1970; Price, 1985; Chen et al., 2014; Diodato et al., 2016). If the stochastic choice of a single receptor in each neuron can be biased by salient odor associations in the environment, this would afford a mechanism to alter receptor representations in the epithelium.

The mechanisms responsible for the increase in the number of OSNs following aversive conditioning are more readily addressed in the sensory epithelium of F0 mice than in the F1 progeny. Elucidation of these local signaling events may then provide insight into the more distant transmission of information to the gametes. The mature olfactory sensory epithelium undergoes constant neurogenesis throughout the life of vertebrates. In mice, the lifespan of a mature OSN is estimated to be 30 days, and new sensory neurons are continually generated by the division of basal stem cells, transit amplification, and

ultimately differentiation to the mature OSN (Liberia et al., 2019). Continual balanced neurogenesis suggests that increases in OSNs upon aversive conditioning could result from the increased birth or enhanced survival of a specific OSN population.

In this study, we performed quantification of OSNs after aversive olfactory learning, corroborating the results of an increase in the OSNs expressing a receptor responsive to the conditioned odor. Moreover, enhanced numbers of these specific OSNs are also observed in the F1 generation. Contrary to previous studies, we do not observe the inheritance of odor-evoked aversion to the conditioned odor in the F1 generation using our behavioral paradigm. We demonstrate that this phenomenon is persistent, as increases in specific OSNs continue for at least 63 days after conditioning. We further demonstrate that a biased increase in specific OSNs after learning is likely to result from the enhanced birth of specific OSNs, suggesting that biased receptor choice underlies this phenomenon in the parent and is epigenetically inherited by their offspring.

RESULTS

In initial experiments, we asked whether we could observe changes in the abundance of receptors responsive to conditioned odors after aversive olfactory learning. The odorant receptor M71 is responsive to the odorant acetophenone, whereas neurons expressing MOR23 are activated by lyral. Homozygous mice modified at the M71 or MOR23 loci to also express GFP allowed for a determination of receptor abundance. These mice were subjected to an aversive olfactory conditioning paradigm in which acetophenone, lyral, or propanol, co-terminating with 0.75mA foot shock, were presented 5 times daily for 3 consecutive days (Fig 1B,C.). The unpaired control group also received odor presentations but experienced a 60-second delay prior to foot shock (Fig 1C.). Only mice in which odorant and shock were paired exhibited conditioned aversive behavior (Supplementary Fig 1B,C,D. Tukey's multiple comparisons. F0 acetophenone unpaired vs. paired P=0.0008. n=10,15. F0 lyral unpaired vs. paired P=0.0057. n=10,15. F0 propanol unpaired vs. paired P<0.0001. n=10,15.). Mouse nasal turbinates were surgically extracted 21 days after the initiation of training and subjected to iDISCO+ tissue clearing to visualize M71- and MOR23-expressing OSNs in transparent intact olfactory epithelia (Fig 1B,D,E. Renier et al., 2016). We then imaged the cleared epithelia using light sheet microscopy and counted the number of M71 or MOR23 OSNs in a fixed volume of tissue using automated spot detection software (Fig 1G,I.).

Importantly, both M71 and MOR23 OSNs are expressed in the same zone of the epithelium, enabling consistent imaging and counting protocols for both OSN populations. Male and female M71-IRES-tauGFP$^{+/+}$ (M71GFP) mice paired with acetophenone exhibited a 33% increase in the number of M71 OSNs 21 days after the initiation of aversive conditioning when compared to unpaired controls (Fig 1H. One-way ANOVA. P<0.0001. Tukey's multiple comparisons. Naïve vs. paired P<0.0001. F0 unpaired vs. paired P<0.0001. n=12,11,12.). Male and female MOR23-IRES-tauGFP$^{+/+}$ (MOR23GFP) mice conditioned with lyral exhibited a 39% increase in MOR23 OSNs when compared to unpaired controls (Fig 1J. One-way ANOVA. P<0.0001. Tukey's multiple comparisons. Naïve vs. paired P=0.0159. F0 unpaired vs. paired P<0.0001. n=9,9,9.). We performed a

series of control experiments to demonstrate that fear conditioning does not lead to a global increase in the number of OSNs per cubic volume in the sensory epithelium. The odorant propanol does not activate M71 sensory neurons (Johnson & Leon, 2000; Jones et al., 2008). When propanol was employed as the conditioned odor in both the paired and unpaired training paradigms, we observed no difference in the number of M71 OSNs between the two groups of mice (Fig 1F. Student's unpaired t-test. Unpaired vs. paired P=0.3009. n=6,7.). These results indicate that olfactory fear conditioning results in a specific increase in the number of cells responsive to the conditioned odor and does not lead to a global increase in all OSNs.

We observe an increase in M71 OSNs 21 days after aversive conditioning with acetophenone. We next asked if this increase persists at later time points (Fig 2A.). At 42 days, we observe a persistent 20% increase (Fig 2B. Tukey's multiple comparisons. 42d unpaired vs. paired P=0.0476. n=8,8.) in the number of M71 OSNs in paired versus unpaired animals and a 30% increase at 63 days (Fig 2B. Tukey's multiple comparisons. 63d unpaired vs. paired P=0.0011. n=4,6.). Since the half-life ($t_{1/2}$) of the mouse olfactory sensory epithelium (the amount of time required for half of the epithelium to regenerate) is approximately 26 days (Holl, 2018), then at 42 days, approximately 67% will have been replaced by newly born neurons, and at 63 days, approximately 81% will have been replaced. The observation that these changes persist at least 63 days after aversive conditioning, together with the reported 26-day half-life for the main olfactory epithelium, suggests that a signaling mechanism must persist despite the fact that the entire sensory epithelium present at the time of conditioning will eventually be regenerated.

We next asked whether the increase in the number of specific OSNs observed following conditioning is inherited by naïve offspring. Ten days after the initiation of aversive training, we bred F0 males from both the paired and unpaired groups with naïve M71GFP$^{+/+}$ or MOR23GFP$^{+/+}$ female mice. Each mating pair was separated ten days after co-housing to ensure that the offspring were never exposed to the conditioned father. Main olfactory epithelia were then collected from the offspring of these matings at 8 weeks of age. The F1 mice were never exposed to acetophenone or lyral, nor had they undergone aversive conditioning. We nonetheless observed a 36% increase in M71 OSNs in both male and female offspring whose fathers experienced paired aversive conditioning with acetophenone when compared with the F1 of fathers that experienced the unpaired training paradigm (Fig 1H. Tukey's multiple comparisons. F1 unpaired vs. paired P<0.0001. n=12,14.). A similar relative increase of 27% was observed in MOR23 OSNs in offspring of fathers that experienced paired aversive conditioning with lyral compared to F1 of unpaired fathers (Fig 1J. Tukey's multiple comparisons. F1 unpaired vs. paired P=0.0368. n=6,6.). These results demonstrate the intergenerational epigenetic inheritance of an olfactory phenotype, namely an increase in specific OSNs in naïve F1 offspring following aversive conditioning in F0.

Previous behavioral studies demonstrated that offspring from fathers that experienced aversive olfactory conditioning exhibit enhanced sensitivity to the conditioned odor in both odor potentiated startle and aversive odor association assays (Dias & Ressler, 2014). Therefore, we asked whether we could detect an aversive behavioral response to either

acetophenone or lyral in the F1 population after aversive training in F0 fathers. In initial experiments, we performed aversive conditioning with either acetophenone or lyral in F0 males and females. Five days after the initiation of training, we placed mice in a 3-chamber arena with the conditioned odor on one side and a control odor (propanol) on the other. F0 mice in the paired group actively avoided the conditioned odor, whereas mice in the unpaired group exhibited no aversion to the conditioned odors (Supplementary Fig 1B,C. Tukey's multiple comparisons. F0 acetophenone unpaired vs. paired P=0.0008. n=10,15. F0 lyral unpaired vs. paired P=0.0057. n=10,15.). Control mice spent roughly equal time exploring the propanol and conditioned odor chambers, whereas the paired mice spent approximately 67% (lyral paired) to 75% (acetophenone paired) of the time exploring the propanol chamber. Importantly, the offspring of F0 fathers that experienced aversive training with acetophenone exhibited no apparent avoidance of the conditioned odor. F1 mice spent equal time in both chambers (Supplementary Fig 1B. Tukey's multiple comparisons. F1 acetophenone unpaired vs. paired P=0.9403. n=4,6.). We note an unexplained result with the offspring of male mice conditioned with propanol. Propanol was behaviorally neutral in the F1 offspring from fathers that experienced paired aversive training with propanol (Supplementary Fig 1D. Tukey's multiple comparisons. Naïve vs. F1 paired P=0.6624. n=25,12.). However, offspring from fathers that had undergone unpaired training exhibited an attraction to propanol (Supplementary Fig 1D. Tukey's multiple comparisons. Naïve vs. F1 unpaired P=0.0001. n=25,5.). Taken together, these results demonstrate that aversive odorant conditioning in the F0 population elicits active avoidance, but suggest that this behavioral phenotype is not transmitted to F1 progeny.

The olfactory epithelium undergoes neurogenesis for the life of the organism. This continual renewal of OSNs suggests a possible mechanism for the observed increase in specific neuron populations responsive to conditioned odors. The increase in M71 and MOR23 cells following aversive training could result from a biased increase in either the birth or survival of specific OSNs. In initial experiments, we examined the relative number of M71 and MOR23 OSNs born during and after aversive training. We injected mice at the onset of training with 5-Ethynyl-2′-deoxyuridine (EdU), a thymidine analog that incorporates into newly synthesized DNA and labels newborn cells. Animals were injected during each of the 3 days of training and for 2 subsequent days (Fig 3A.). Epithelia were examined to determine the number of EdU-labeled M71 and MOR23 OSNs 21 days after the initiation of paired and unpaired aversive training (Fig 3A.). Since EdU has a half-life of approximately 35 minutes (Cheraghali et al., 1995), analysis of EdU 16 days after the cessation of EdU exposure reflects a pulse-chase, allowing us to quantify a subset of the neurons born during the 5 days following the initiation of aversive conditioning (Fig 3B.).

The number of newborn M71 cells (EdU-labeled) out of total M71 cells is 1.24 ± 0.29% in naïve mice, 2.91 ± 0.56% after the unpaired paradigm, and 7.61 ± 0.53% following paired aversive training with acetophenone (Fig 3D. One-way ANOVA. P<0.0001. Tukey's multiple comparisons. Naïve vs. paired P<0.0001. Unpaired vs. paired P<0.0001. n=6,6,6.). When lyral is used as the conditioned odor, the number of newborn MOR23 cells out of total MOR23 cells is 0.29 ± 0.06% in naïve mice, 0.55 ± 0.09% after the unpaired paradigm, and 1.11 ± 0.21% following paired aversive training (Fig 3E. One-way

ANOVA. P=0.0120. Tukey's multiple comparisons. Naïve vs. paired P=0.0154. Unpaired vs. paired P=0.0653. n=4,6,8.). These observations suggest that aversive learning results in a significant increase in the number of newborn M71 and MOR23 cells when comparing the paired and unpaired paradigms. The observation that the percentage of newborn M71 cells is 4-5 times that of MOR23 may simply reflect differences in the birth rates of the two cell populations.

We scored the number of EdU-labeled M71 and MOR23 OSNs 16 days after the cessation of EdU exposure. Since the differentiation of a newborn cell to a mature olfactory neuron requires about 7-10 days (Miragall & Graziadei, 1982; Liberia et al., 2019), these data strongly suggest that aversive training results in a specific increase in the birth of new cells responsive to the conditioned odor. Experiments suggest that an enhanced rate of survival is not responsible for the observed increase in specific OSNs. If EdU is administered prior to the onset of training, an increase in the number of EdU+ cells would reflect enhanced survival rather than increased birth. However, daily exposure to EdU for 5 days 12 days prior to conditioning does not reveal a relative increase in the frequency of EdU+ M71 or MOR23 cells when comparing the paired and unpaired paradigms (data not shown). Taken together, these data strongly suggest that the specific increase in cells responsive to the conditioned odor is a consequence of a relative increase in the birth of new cells expressing the M71 and MOR23 receptors.

DISCUSSION

We used tissue-clearing techniques and light-sheet microscopy to demonstrate an increase in olfactory sensory neurons (OSNs) expressing the receptor for an aversively conditioned odor. Moreover, enhanced cell numbers to the conditioned odor were observed in naïve offspring. These data are in accord with findings that employ other cellular visualization techniques (Dias & Ressler, 2014; Aoued et al., 2019; Aoued et al., 2020). In F0, this increase is stable for 63 days, a time by which the vast majority of the cells present during aversive training have been replaced by newborn sensory neurons. The increase in F0 results, in part, from the contribution of newborn neurons responsive to the conditioned odor, demonstrating a biasing of olfactory receptors during OSN development. The sustained increase in F0, along with the inheritance in F1, suggests that there is a stable signal that is responsible for the induction, maintenance, and inheritance of the increase in OSNs responsive to the paired odor.

The stochastic choice of olfactory receptors may provide an opportunity to alter the representation of receptors in order to allow an organism to adapt to the environment. Changes in the number of OSNs may lead to an increase in sensitivity of the paired odor. A change in OSN number may also lead to increased inputs to downstream sensory areas. Such perceptual changes have been reported in the motor, visual, olfactory, and auditory systems, where topographical arrangements at the primary sensory cortex are modulated in certain fear conditioning paradigms in mammals (Ressler et al., 1994; Vassar et al., 1994; Mombaerts et al., 1996; Lai et al., 2018; Xu et al., 2019; Li et al., 2019), although this has not yet been demonstrated intergenerationally. We speculate that the increase in neurons responsive to the conditioned odor will enhance the

sensitivity or discrimination of that odorant, including in naïve offspring. These findings position future studies to uncover the mechanism by which olfactory receptor bias is communicated within the main olfactory epithelium, to the germline, and, moreover, maintained during the development of offspring. What remains to be uncovered are the mechanisms to bias the choice of specific receptors in the main olfactory epithelium and how the information governing the biasing of receptor choice is transferred to the gametes.

In mice, the paternal transmission of epigenetic information has been observed following metabolic disturbances, social stress, and exposure to drugs and toxins (Huypens et al., 2016). High-fat or low-protein diets, as well as caloric restriction in the father, results in metabolic disturbances in the offspring, even after *in vitro* fertilization (Carone et al., 2010; Chen et al., 2016). Parental stressors, such as chronic defeat or maternal separation, result in hormonal disturbances and behavioral phenotypes in the offspring (Deitz et al., 2011; Morgan & Bale, 2011; Gapp et al., 2014). Finally, toxins and addictive drugs result in an array of metabolic disturbances in the F1 population that recapitulate the paternal state (Toussaint et al., 2022). These paternal stressors are associated with metabolic and hormonal disturbances that can readily act at a distance to affect the gamete. It has been demonstrated in male gametogenesis that extracellular vesicles in the testes transmit an RNA payload as they fuse with maturing sperm (Rando, 2016; Sharma et al., 2018; Morgan et al., 2019; Chan et al., 2020). Such studies provide insights into a mechanism by which an olfactory sensory experience paired with fear learning could transmit receptor-specific information from one generation to the next.

Our study elaborates on a function of sensory systems in which a learned adaptation can influence future generations. Thus, the distinction between innate and learned behaviors may be fundamentally flexible — learned adaptations in the parent may have the potential to become innate in their offspring. Understanding the mechanisms of inherited adaptation will provide insight for interventions when these changes no longer serve as adaptive to the organism.

AUTHOR CONTRIBUTIONS

C.W.L., Y.R.A., and B.J.M. designed the study. C.W.L., E.C.B.J., H.S.L., A.K., and B.J.M. conducted iDISCO+ brain clearing and cell counts. C.W.L. and Y.R.A. conducted EdU histology. C.W.L., Y.R.A., E.C.B.J., H.S.L., and A.K. conducted behavioral experiments. C.W.L. and Y.R.A. designed graphics. C.W.L. designed figures and graphical abstract. All authors analyzed data. C.W.L., Y.R.A., R.A., and B.J.M. wrote the manuscript.

ACKNOWLEDGEMENTS

The authors have no competing interests in this work. Mice were treated in compliance with the rules and regulations of Columbia University IACUC under protocol number #AABL8552. We thank the past and current members of the Marlin Lab for critical discussions and inputs on the manuscript. We thank Dr. Richard Axel, Dr. Stavros

Lomvardas, Dr. Carol Mason, Dr. Robert Froemke, Dr. Ishmail Abdus-Saboor, Dr. Ismail Ahmed, and Dr. Joseph Jones Marlin for their comments, discussion, and technical assistance. We thank A.I.S.C, A.M., and V.L.F.N. for their support. We thank Stellate Communications for assistance with figure production and preparation of the manuscript. Imaging was performed with support from the Zuckerman Institute's Cellular Imaging platform and the National Institutes of Health (NIH 1S10OD023587-01). This study was supported by the Simons Foundation (B.J.M.), the UNCF, Bristol-Myers Squibb EE Just Fellowship (B.J.M.), and a NARSAD Young Investigator Grant (B.J.M.).

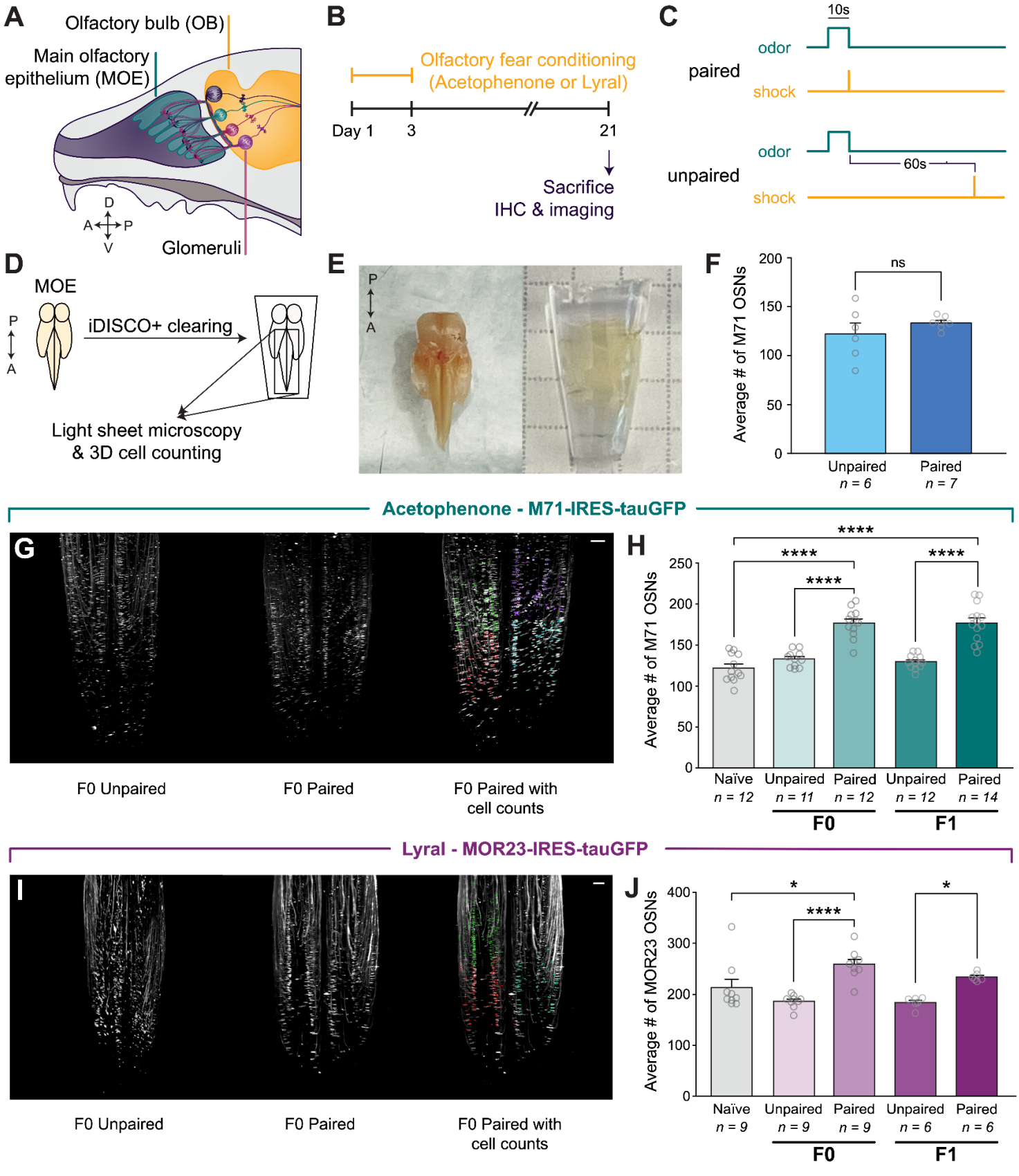

Figure 1. Olfactory fear conditioning leads to an increase in conditioned-odor-responsive cells in parents (F0) that is heritable (F1)

a. Schematic representation of the mouse main olfactory epithelium and olfactory bulb. MOE: main olfactory epithelium. OB: olfactory bulb. **b.** Timeline of olfactory fear conditioning and MOE collection. **c.** Experimental paradigms for olfactory fear conditioning groups. Mice in the paired condition received a footshock that co-terminated with odor presentation, while mice in the unpaired condition received a footshock 60 seconds after odor presentation. **d.** Schematic demonstrating the process by which cells of interest in the MOE were quantified. Epithelia from both M71-IRES-tauGFP$^{+/+}$ and MOR23-IRES-tauGFP$^{+/+}$ adult mice were cleared using the iDISCO+ tissue-clearing protocol. Samples were imaged on a light sheet microscope and analyzed using Imaris spot detection software. **e.** Images of the MOE before (left) and after (right) optical tissue clearing. **f.** The average number of M71 olfactory sensory neurons in a 350^3 um^3 cube of the epithelium in the propanol unpaired (light blue) and propanol paired (dark blue) conditions (Student's unpaired t-test. Unpaired vs. paired P=0.3009. n=6,7.). **g.** Example images of M71 OSNs in zone 1 of cleared MOE from both the unpaired (left) and paired (middle) conditions. Example image of an MOE with the counted cells represented by colored dots (right). Each set of colors represents a distinct counting cube. Scale bar: 200um. **h.** Graph showing the differences between the average number of M71 OSNs in a 350^3 um^3 cube of epithelium of naive (gray), acetophenone unpaired (lighter green), and acetophenone paired (darker green) conditions in F0 and F1 (One-way ANOVA. P<0.0001. Tukey's multiple comparisons. Naïve vs. F0 paired P<0.0001. F0 unpaired vs. paired P<0.0001. Naïve vs. F1 paired P<0.0001. F1 unpaired vs. paired P<0.0001. n=12,11,12,12,14.). **i.** Example images of MOR23 OSNs in zone 1 of cleared MOE from both the unpaired (left) and paired (middle) conditions. Example image of an MOE with the counted cells represented by colored dots (right). Scale bar: 200um. **j.** Graph showing the differences between the average number of MOR23 OSNs in a 350^3 um^3 cube of epithelium in naive (gray), lyral unpaired (lighter purple), and lyral paired (darker purple) conditions in F0 and F1 (One-way ANOVA. P<0.0001. Tukey's multiple comparisons. Naïve vs. F0 paired P=0.0159. F0 unpaired vs. paired P<0.0001. F1 unpaired vs. paired P=0.0368. n=9,9,9,6,6.).

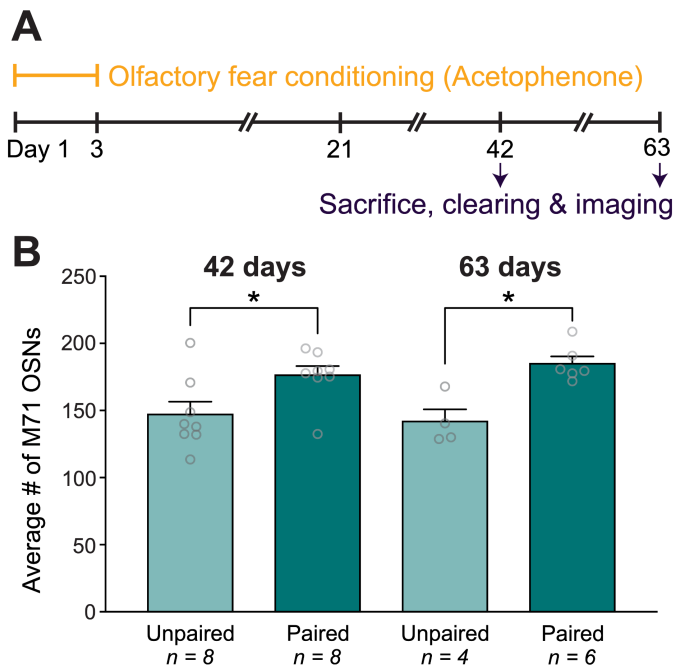

Figure 2. Conditioned-odor-responsive cell increase is sustained through at least 9 weeks of cell turnover

a. Timeline of olfactory fear conditioning and extended MOE collection time points. **b.** The average number of M71 OSNs in a 350^3 um^3 cube of epithelium of unpaired (light green) and paired (dark green) mice, 42 or 63 days post-conditioning (One-way ANOVA. P=0.0033. Tukey's multiple comparisons. 42d unpaired vs. paired P=0.0476. 63d unpaired vs. paired P=0.0011. n=8,8,4,6.).

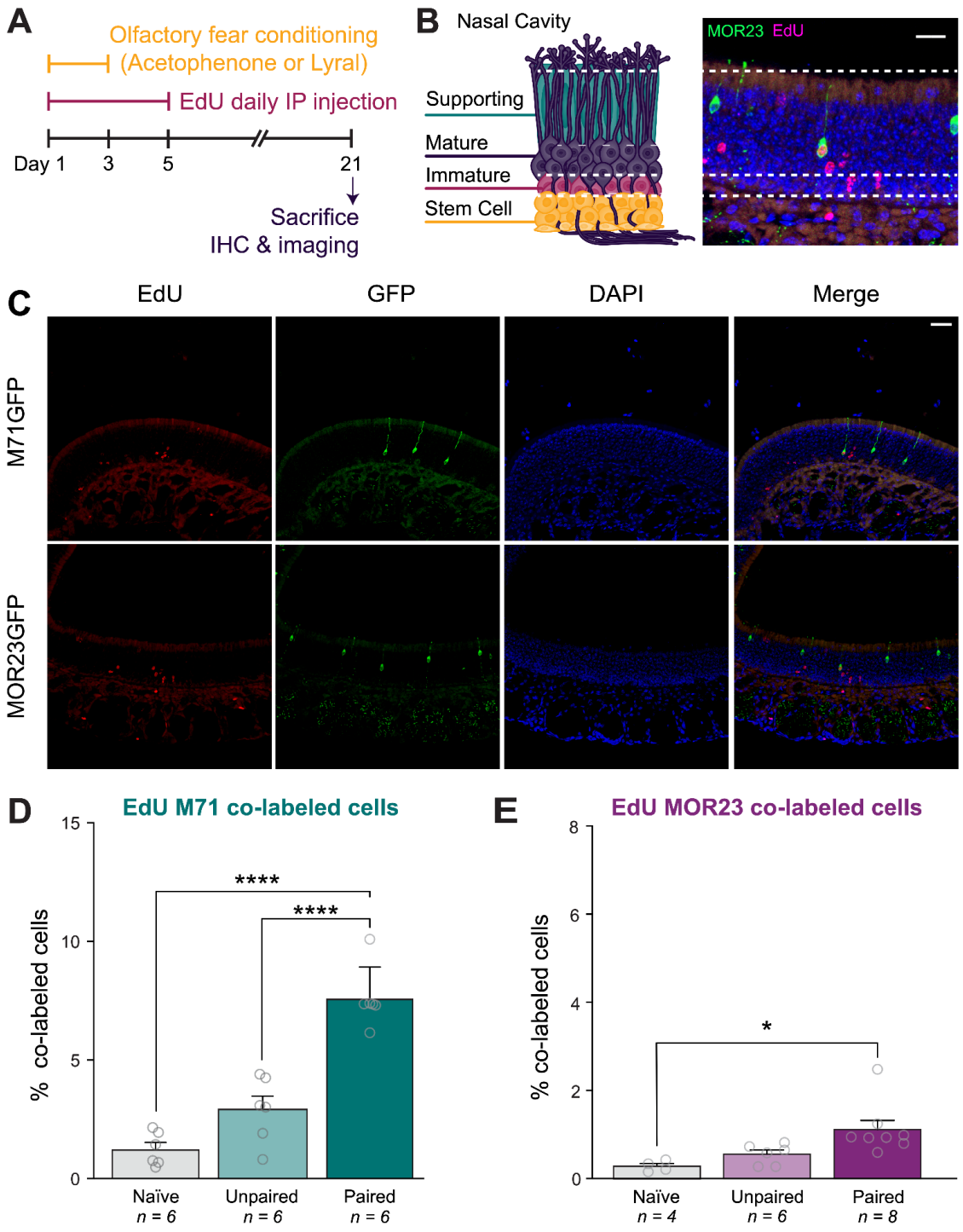

Figure 3. Olfactory fear conditioning biases olfactory receptor choice toward conditioned-odor-responsive cell-specific identities

a. Timeline of olfactory fear conditioning, EdU injections, and MOE collection. **b.** Schematic representation of the distinct layers of the MOE, showing the stem cell, immature OSN, and mature OSN populations (left). Representative image of the MOE from an MOR23GFP$^{+/+}$ mouse showing EdU-positive cells (red) and a newborn (EdU+) MOR23 OSN (green). Scale bar: 20 um. **c.** Representative images showing staining of

EdU (red, first column), endogenous GFP (green, second column), DAPI (blue, third column), and the merged channels (fourth column) in both M71GFP$^{+/+}$ and MOR23GFP$^{+/+}$ MOE. Scale bar: 40um. **d.** Percentage of EdU-positive M71 OSNs in naïve, unpaired, and paired groups (One-way ANOVA. P<0.0001. Tukey's multiple comparisons. Naïve vs. paired P<0.0001. Unpaired vs. paired P<0.0001. n=6,6,6.). **e.** Percentage of EdU-positive MOR23 OSNs in naïve, unpaired, and paired groups (One-way ANOVA. P=0.0120. Tukey's multiple comparisons. Naïve vs. paired P=0.0154. Unpaired vs. paired P=0.0653. n=4,6,8.).

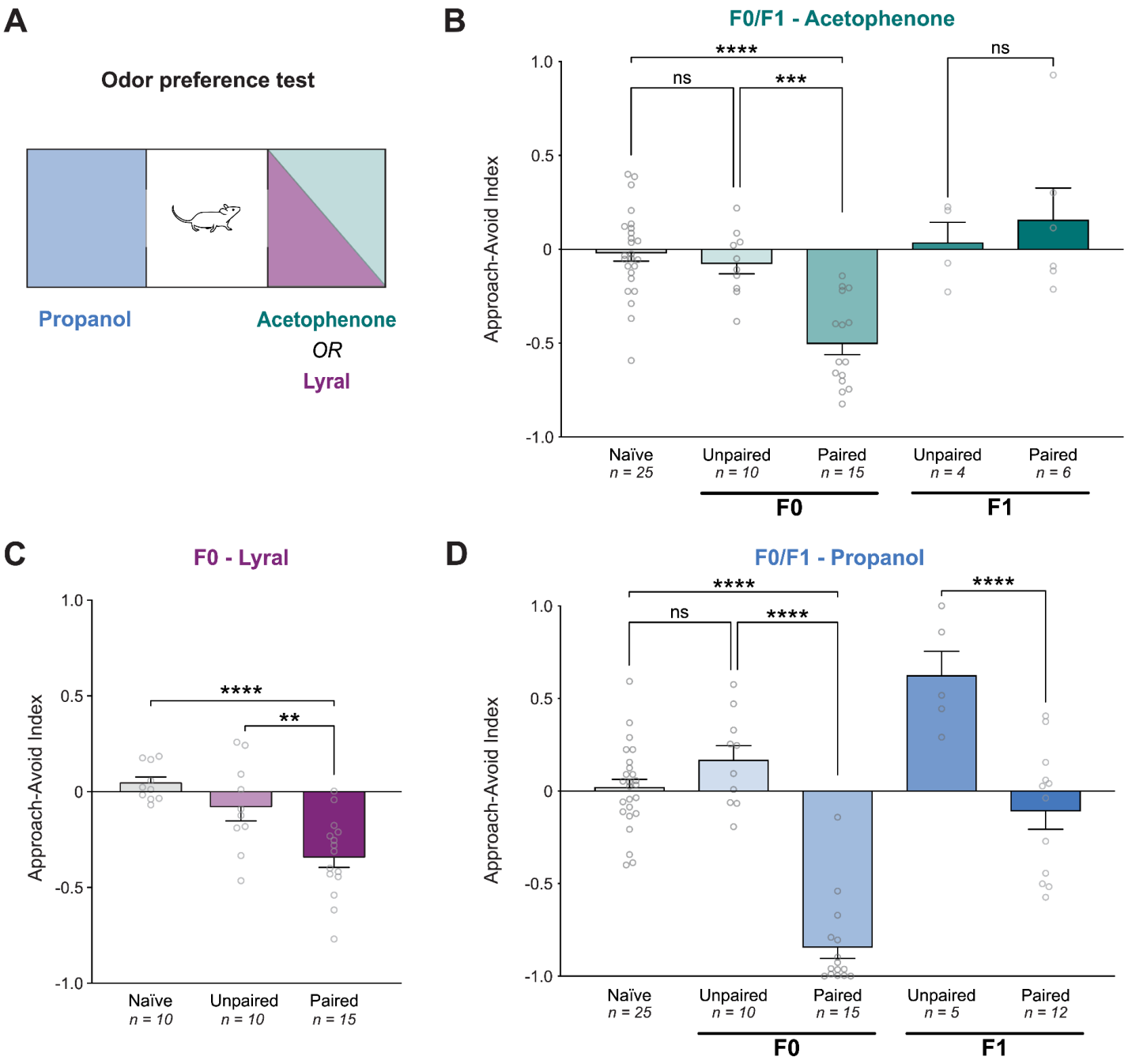

Supplementary Figure 1. Olfactory fear conditioning leads to active avoidance behavior in parents (F0) that is not heritable (F1)

a. Schematic of the three-chamber behavioral approach-avoidance assay. **b.** The approach-avoid index for acetophenone in the naïve (gray), unpaired (lighter green), and paired (darker green) conditions in F0 and F1 (One-way ANOVA. P<0.0001. Tukey's multiple comparisons. Naïve vs. F0 paired P<0.0001. F0 unpaired vs. paired P=0.0008. F1 unpaired vs. paired P=0.6161. n=25,10,15,4,6.). Positive values indicate approach, and negative values indicate avoidance. **c.** The approach-avoid index for lyral in the naïve (gray), unpaired (light purple), and paired (dark purple) conditions in F0 (One-way

ANOVA. P<0.0001. Tukey's multiple comparisons. Naïve vs. paired P<0.0001. Unpaired vs. paired P=0.0057. n=10,10,15.). **d.** The approach-avoid index for propanol in the naive (gray), unpaired (lighter blue), and paired (darker blue) conditions in F0 and F1 (One-way ANOVA. P<0.0001. Tukey's multiple comparisons. Naïve vs. F0 paired P<0.0001. F0 unpaired vs. paired P<0.0001. Naïve vs. F1 unpaired P=0.0001. F1 unpaired vs. paired P<0.0001. n=25,10,15,5,12.).

Supplementary Figure 2 (*File attached in Supplementary Material*). Cleared zone 1 olfactory epithelium counting method

a. Representative image of zone 1 of a cleared MOE from an M71GFP$^{+/+}$ unpaired mouse. M71 OSNs are visualized in white. Scale bar: 200um. **b.** The same cleared olfactory epithelium as the left, but with 4 sets of automated cell counts overlaid. Each color represents a different counting cube. **c.** The 4 sets of automated cell counts, minus the tissue image. The average of all sets of cell counts was used for each data point, with a minimum of 3 sets for inclusion.

Supplementary Figure 3 (*Files attached in Supplementary Material*). Approach avoidance videos

a. Representative video of odor preference behavior assay. Mouse has undergone unpaired olfactory fear conditioning with acetophenone. Left chamber: propanol. Right chamber: acetophenone. **b.** Representative video of odor preference behavior assay. Mouse has undergone paired olfactory fear conditioning with acetophenone. Left chamber: propanol. Right chamber: acetophenone.

Supplementary Figure 4 (*Files attached in Supplementary Material*). Cleared olfactory epithelium videos

a. b. c. Representative videos of zone 1 of a cleared MOE from an M71GFP$^{+/+}$ unpaired mouse. M71 OSNs are visualized in white. (**c)** shows coronal slices of a section of zone 1 from anterior to posterior. The top of the video is dorsal, and the bottom is ventral. Scale indicated in each video. **d. e. f.** Representative videos of zone 1 of a cleared MOE from an M71GFP$^{+/+}$ paired mouse. M71 OSNs are visualized in white. (**f)** shows coronal slices of a section of zone 1 from anterior to posterior. The top of the video is dorsal, and the bottom is ventral. Scale indicated in each video.

MATERIALS AND METHODS

Mice

All procedures were approved by the Columbia University Institutional Animal Care and Use Committee under protocol #AABL8552. All mice were housed with a 12 hr light/12 hr dark cycle and fed ad libitum. M71-IRES-tauGFP (Stock #006676), MOR23-IRES-tauGFP (Stock #006643), and C57BL/6J (Stock #000664) mice were obtained from The Jackson Laboratory or gifted from the Lomvardas and the Axel laboratories.

Olfactory fear conditioning

8-12 week-old male and female mice were trained to associate acetophenone (Sigma-Aldrich, 42163), lyral (IFF, 00129214), or propanol (Sigma-Aldrich, I9516) with 0.75mA foot shocks. Odors were diluted to 10% v/v in mineral oil (Fisher, O121-1). The mice were trained on 3 consecutive days, with each training day consisting of 5 presentations of odor for 10 seconds. For mice in the paired condition, the odor presentations were co-terminated with a 0.75mA foot shock. For mice in the unpaired condition, there was a 60-second delay between the odor presentation and foot shock (Fig 1C.). Olfactory fear conditioning boxes, olfactometers, and software were obtained from Med Associates. Mice were randomly assigned to experimental conditions.

Odor preference behavioral testing

At least 1 day following olfactory fear conditioning, conditioned mice were assayed in a custom-built acrylic three-chamber box to assess odor avoidance behavior (Supplementary Fig 1A.). The conditioned and control odors were assigned randomly to either side. Odors were diluted to 1% v/v in mineral oil for all odor preference assays, and flowmeters were set to equal flow rates. The three-chamber box included vacuum ports both in the center chamber, as well as on either side of the center chamber doorways in the side chambers to ensure each experimental odor was restricted to its chamber. The mice were habituated to the center chamber for 1 minute prior to the start of the test, and then the doors to both chambers were lifted to initiate the assay. Mice were recorded roaming freely throughout the three-chamber box for 10 minutes. The odor avoidance index was manually scored by blinded counters as approach-avoidance index = (time spent on control odor side - time spent on conditioned odor side) / total time spent on either side. Animals sampled each chamber for a minimum of 3 seconds for inclusion.

Tissue clearing

MOEs were perfused, dissected, and processed according to the iDISCO+ protocol as described in Renier et al. (2016). Whole MOEs were processed in 5mL volumes. Samples were postfixed in 4% paraformaldehyde in 1X PBS (Electron Microscopy Sciences, 15710-S) overnight at 4°C. The following day, they were washed with 1X PBS (3 x 30

minutes), gradually dehydrated with methanol (MeOH; Sigma-Aldrich, 322415) over 5 hours, and incubated in 66% dichloromethane (DCM; Sigma-Aldrich, 270997)/33% MeOH overnight. The samples were washed in 100% MeOH the following day, chilled at 4°C, bleached in 5% hydrogen peroxide (Sigma-Aldrich, 216763) in MeOH overnight at 4°C, and then gradually rehydrated the next day. Samples were permeabilized for 2 days and blocked in 6% goat serum (Jackson ImmunoResearch, 005-000-121) for 2 days at 37°C. Next, they were labeled with a 1:2000 dilution of primary chicken anti-GFP antibody (Aves Labs, GFP-1020) for 3 days at 37°C, washed for 1 day (5 x 1 hour), and labeled with a 1:1000 dilution of secondary goat anti-chicken Alexa Fluor 647 antibody (Invitrogen, A-21449) for 3 days at 37°C. Due to the fragility of the nasal turbinates housing the majority of zone 1, samples were embedded in 4% agarose (Invitrogen, 16500100) prior to final dehydration (Fig 1E.). Lastly, the embedded samples were incubated in 66% DCM/33% MeOH for 3 hours, rinsed twice with 100% DCM, and transferred to dibenzyl ether (Sigma-Aldrich, 33630) for final clearing.

Lightsheet imaging

Images were collected with a light-sheet ultramicroscope (Ultramicroscope II, LaVision BioTec) at 2.0X magnification using a 640 nm laser and a z-step size of 2.0um. All cleared tissue images were acquired with tissue submerged in dibenzyl ether (DBE). Laser intensity was set between 55% and 75% to prevent oversaturated pixels and photobleaching. The working distance of the microscope allowed for complete visualization of both left and right turbinates containing zone 1 OSNs (Fig 1G,I.). The light-sheet microscope was provided by Cellular Imaging at the Zuckerman Institute (NIH 1S10OD023587-01).

Imaris 3D cell quantification

All quantification was performed in a double-blind manner. The image stack of GFP+ olfactory sensory neurons in the 647 nm channel was analyzed using Imaris software. The average number of olfactory sensory neurons was measured using the spot detection tool on 350^3 um^3 cubes of zone 1 tissue, with a requirement of at least 3 cubes per sample for inclusion. The decision to measure an average number of cells within a fixed volume, as opposed to the total number of cells in the turbinates, accounted for potential tissue loss and differences in tissue volumes/shapes across samples. The spot detection was set to a 16.3um estimated diameter and was based on Imaris' quality threshold, which compares the intensities at the centers of the candidate spots. The quality threshold varied slightly across samples to adjust for signal quality and axon brightness (to minimize counting spots on axons), but was held consistent within every sample.

5-Ethynyl-2′-deoxyuridine (EdU) injections

10mM EdU (Invitrogen, E10187) was administered to male and female 8-12 week-old M71GFP$^{+/+}$ and MOR23GFP$^{+/+}$ mice through a series of daily 0.01mL/g intraperitoneal injections. Injections were administered 15 minutes prior to olfactory fear conditioning on each of the 3 days of conditioning, plus 2 additional days around the same time conditioning had been performed (Fig 3A.).

EdU click chemistry

Mice were transcardially perfused with ice-cold 4% PFA (Electron Microscopy Sciences, 15710-S) in 1X PBS. Main olfactory epithelia were surgically dissected, incubated in 4% PFA overnight, and cryoprotected in 30% sucrose (Sigma-Aldrich, S0389). Main olfactory epithelia were frozen in OCT (Fisher, 23-730-571) and stored at -20°C until sectioning. Tissue was sliced into 20um sections, mounted directly onto Fisher Superfrost Plus glass slides (Fisher, 12-550-15), and stored at -80°C until staining. At the time of staining, slides were acclimated to room temperature, washed with PBST (0.1% Triton X-100 in 1X PBS; 3 x 5 minutes; Sigma-Aldrich, X100), and incubated with Click-iT Plus EdU reaction cocktail (Alexa Fluor 555; 30 minutes; Invitrogen, C10638). Sections were washed again with PBST (3 x 5 minutes), with the last wash including 1:10,000 DAPI (Invitrogen, D1306), and then coverslipped using Vectashield Plus mounting medium (Vector Labs H-1900) and sealed with nail polish.

Confocal image acquisition

Slides were imaged using a Zeiss Upright LSM 880 Confocal microscope and Zen Black software (Zeiss). All co-labeling images were acquired in z-stacks to ensure accuracy in co-labeling determination.

Statistics

All data points were included in analysis. A significance threshold of $p<0.05$ was used for all statistical analyses. Statistical analyses of comparisons between 2+ groups were performed using a standard one-way ANOVA with Tukey's multiple comparisons for individual comparisons, and comparisons between 2 groups were performed using Student's unpaired t-tests. Descriptive statistics used standard error of the mean (S.E.M.) to estimate error. Percent differences between 2 groups were calculated by comparing the mean of each group. All statistical analysis was performed using Prism 9 (GraphPad) software.

REFERENCES

Aoued, Hadj S., Soma Sannigrahi, Nandini Doshi, Filomene G. Morrison, Hannah Linsenbaum, Sarah C. Hunter, Hasse Walum, et al. "Reversing Behavioral, Neuroanatomical, and Germline Influences of Intergenerational Stress." *Biological Psychiatry* 85, no. 3 (01 2019): 248–56. https://doi.org/10.1016/j.biopsych.2018.07.028.

Aoued, Hadj S., Soma Sannigrahi, Sarah C. Hunter, Nandini Doshi, Zakia S. Sathi, Anthony W. S. Chan, Hasse Walum, and Brian G. Dias. "Proximate Causes and Consequences of Intergenerational Influences of Salient Sensory Experience." *Genes, Brain and Behavior* 19, no. 4 (2020): e12638. https://doi.org/10.1111/gbb.12638.

Buck, L., and R. Axel. "A Novel Multigene Family May Encode Odorant Receptors: A Molecular Basis for Odor Recognition." *Cell* 65, no. 1 (April 5, 1991): 175–87. https://doi.org/10.1016/0092-8674(91)90418-x.

Carone, Benjamin R., Lucas Fauquier, Naomi Habib, Jeremy M. Shea, Caroline E. Hart, Ruowang Li, Christoph Bock, et al. "Paternally Induced Transgenerational Environmental Reprogramming of Metabolic Gene Expression in Mammals." *Cell* 143, no. 7 (December 23, 2010): 1084–96. https://doi.org/10.1016/j.cell.2010.12.008.

Chan, Jennifer C., Christopher P. Morgan, N. Adrian Leu, Amol Shetty, Yasmine M. Cisse, Bridget M. Nugent, Kathleen E. Morrison, et al. "Reproductive Tract Extracellular Vesicles Are Sufficient to Transmit Intergenerational Stress and Program Neurodevelopment." *Nature Communications* 11, no. 1 (March 20, 2020): 1499. https://doi.org/10.1038/s41467-020-15305-w.

Chen, Chien-Fu F., Dong-Jing Zou, Clara G. Altomare, Lu Xu, Charles A. Greer, and Stuart J. Firestein. "Nonsensory Target-Dependent Organization of Piriform Cortex." *Proceedings of the National Academy of Sciences* 111, no. 47 (November 25, 2014): 16931–36. https://doi.org/10.1073/pnas.1411266111.

Chen, Qi, Menghong Yan, Zhonghong Cao, Xin Li, Yunfang Zhang, Junchao Shi, Gui-hai Feng, et al. "Sperm TsRNAs Contribute to Intergenerational Inheritance of an Acquired Metabolic Disorder." *Science* 351, no. 6271 (January 22, 2016): 397–400. https://doi.org/10.1126/science.aad7977.

Cheraghali, A. M., R. Kumar, E. E. Knaus, and L. I. Wiebe. "Pharmacokinetics and Bioavailability of 5-Ethyl-2'-Deoxyuridine and Its Novel (5R,6R)-5-Bromo-6-Ethoxy-5,6-Dihydro Prodrugs in Mice." *Drug Metabolism and Disposition* 23, no. 2 (February 1, 1995): 223–26.

Chess, Andrew, Itamar Simon, Howard Cedar, and Richard Axel. "Allelic Inactivation Regulates Olfactory Receptor Gene Expression." *Cell* 78, no. 5 (September 9, 1994): 823–34. https://doi.org/10.1016/S0092-8674(94)90562-2.

Dalton, Ryan P., David B. Lyons, and Stavros Lomvardas. "Co-Opting the Unfolded Protein Response to Elicit Olfactory Receptor Feedback." *Cell* 155, no. 2 (October 10, 2013): 321–32. https://doi.org/10.1016/j.cell.2013.09.033.

Dias, Brian G, and Kerry J Ressler. "Parental Olfactory Experience Influences Behavior and Neural Structure in Subsequent Generations." *Nature Neuroscience* 17, no. 1 (January 2014): 89–96. https://doi.org/10.1038/nn.3594.

Dietz, David M., Quincey Laplant, Emily L. Watts, Georgia E. Hodes, Scott J. Russo, Jian Feng, Ronald S. Oosting, Vincent Vialou, and Eric J. Nestler. "Paternal Transmission of Stress-Induced Pathologies." *Biological Psychiatry* 70, no. 5 (September 1, 2011): 408–14. https://doi.org/10.1016/j.biopsych.2011.05.005.

Diodato, A., M. Ruinart De Brimont, Y.S. Yim, N. Derian, S. Perrin, J. Pouch, D. Klatzmann, S. Garel, G.B. Choi, and A. Fleischmann. "Molecular Signatures of Neural Connectivity in the Olfactory Cortex." *Nature Communications* 7 (2016). https://doi.org/10.1038/ncomms12238.

Fitz-James, Maximilian H., and Giacomo Cavalli. "Molecular Mechanisms of Transgenerational Epigenetic Inheritance." *Nature Reviews Genetics* 23, no. 6 (June 2022): 325–41. https://doi.org/10.1038/s41576-021-00438-5.

Gapp, Katharina, Ali Jawaid, Peter Sarkies, Johannes Bohacek, Pawel Pelczar, Julien Prados, Laurent Farinelli, Eric Miska, and Isabelle M. Mansuy. "Implication of Sperm RNAs in Transgenerational Inheritance of the Effects of Early Trauma in Mice." *Nature Neuroscience* 17, no. 5 (May 2014): 667–69. https://doi.org/10.1038/nn.3695.

Greer, Eric L., Travis J. Maures, Duygu Ucar, Anna G. Hauswirth, Elena Mancini, Jana P. Lim, Bérénice A. Benayoun, Yang Shi, and Anne Brunet. "Transgenerational Epigenetic Inheritance of Longevity in Caenorhabditis Elegans." *Nature* 479, no. 7373 (November 2011): 365–71. https://doi.org/10.1038/nature10572.

Holl, Anna-Maria. "Survival of Mature Mouse Olfactory Sensory Neurons Labeled Genetically Perinatally." *Molecular and Cellular Neurosciences* 88 (April 2018): 258–69. https://doi.org/10.1016/j.mcn.2018.02.005.

Huypens, Peter, Steffen Sass, Moya Wu, Daniela Dyckhoff, Matthias Tschöp, Fabian Theis, Susan Marschall, Martin Hrabě de Angelis, and Johannes Beckers. "Epigenetic Germline Inheritance of Diet-Induced Obesity and Insulin Resistance." *Nature Genetics* 48, no. 5 (May 2016): 497–99. https://doi.org/10.1038/ng.3527.

Jiang, Yue, Naihua Natalie Gong, Xiaoyang Serene Hu, Mengjue Jessica Ni, Radhika Pasi, and Hiroaki Matsunami. "Molecular Profiling of Activated Olfactory Neurons Identifies Odorant Receptors for Odors in Vivo." *Nature Neuroscience* 18, no. 10 (October 2015): 1446–54. https://doi.org/10.1038/nn.4104.

Johnson, Brett A., and Michael Leon. "Modular Representations of Odorants in the Glomerular Layer of the Rat Olfactory Bulb and the Effects of Stimulus Concentration." *Journal of Comparative Neurology* 422, no. 4 (2000): 496–509. https://doi.org/10.1002/1096-9861(20000710)422:4<496::AID-CNE2>3.0.CO;2-4.

Jones, Seth V., Dennis C. Choi, Michael Davis, and Kerry J. Ressler. "Learning-Dependent Structural Plasticity in the Adult Olfactory Pathway." *The Journal of Neuroscience* 28, no. 49 (December 3, 2008): 13106–11. https://doi.org/10.1523/JNEUROSCI.4465-08.2008.

Lai, Cora Sau Wan, Avital Adler, and Wen-Biao Gan. "Fear Extinction Reverses Dendritic Spine Formation Induced by Fear Conditioning in the Mouse Auditory Cortex." *Proceedings of the National Academy of Sciences* 115, no. 37 (September 11, 2018): 9306–11. https://doi.org/10.1073/pnas.1801504115.

Li, Zhihan, An Yan, Kun Guo, and Wu Li. "Fear-Related Signals in the Primary Visual Cortex." *Current Biology* 29, no. 23 (December 2, 2019): 4078-4083.e2. https://doi.org/10.1016/j.cub.2019.09.063.

Liberia, Teresa, Eduardo Martin-Lopez, Sarah J. Meller, and Charles A. Greer. "Sequential Maturation of Olfactory Sensory Neurons in the Mature Olfactory Epithelium." *Eneuro* 6, no. 5 (September 2019): ENEURO.0266-19.2019. https://doi.org/10.1523/ENEURO.0266-19.2019.

Linden, Carl J. van der, Pooja Gupta, Ashraful Islam Bhuiya, Kelci R. Riddick, Kawsar Hossain, and Stephen W. Santoro. "Olfactory Stimulation Regulates the Birth of Neurons That Express Specific Odorant Receptors." *Cell Reports* 33, no. 1 (October 6, 2020): 108210. https://doi.org/10.1016/j.celrep.2020.108210.

Lomvardas, Stavros, Gilad Barnea, David J. Pisapia, Monica Mendelsohn, Jennifer Kirkland, and Richard Axel. "Interchromosomal Interactions and Olfactory Receptor Choice." *Cell* 126, no. 2 (July 28, 2006): 403–13. https://doi.org/10.1016/j.cell.2006.06.035.

Lyons, David B., William E. Allen, Tracie Goh, Lulu Tsai, Gilad Barnea, and Stavros Lomvardas. "An Epigenetic Trap Stabilizes Singular Olfactory Receptor Expression." *Cell* 154, no. 2 (July 18, 2013): 325–36. https://doi.org/10.1016/j.cell.2013.06.039.

Miragall, F., and G. A. Monti Graziadei. “Experimental Studies on the Olfactory Marker Protein. II. Appearance of the Olfactory Marker Protein during Differentiation of the Olfactory Sensory Neurons of Mouse: An Immunohistochemical and Autoradiographic Study.” Brain Research 239, no. 1 (May 6, 1982): 245–50. https://doi.org/10.1016/0006-8993(82)90846-0.

Mombaerts, Peter, Fan Wang, Catherine Dulac, Steve K. Chao, Adriana Nemes, Monica Mendelsohn, James Edmondson, and Richard Axel. “Visualizing an Olfactory Sensory Map.” *Cell* 87, no. 4 (November 15, 1996): 675–86. https://doi.org/10.1016/S0092-8674(00)81387-2.

Moore, Rebecca S., Rachel Kaletsky, Chen Lesnik, Vanessa Cota, Edith Blackman, Lance R. Parsons, Zemer Gitai, and Coleen T. Murphy. “The Role of the Cer1 Transposon in Horizontal Transfer of Transgenerational Memory.” *Cell* 184, no. 18 (September 2, 2021): 4697-4712.e18. https://doi.org/10.1016/j.cell.2021.07.022.

Morgan, Christopher P., and Tracy L. Bale. “Early Prenatal Stress Epigenetically Programs Dysmasculinization in Second-Generation Offspring via the Paternal Lineage.” *Journal of Neuroscience* 31, no. 33 (August 17, 2011): 11748–55. https://doi.org/10.1523/JNEUROSCI.1887-11.2011.

Morgan, Christopher P., Jennifer C Chan, and Tracy L. Bale. “Driving the Next Generation: Paternal Lifetime Experiences Transmitted via Extracellular Vesicles and Their Small RNA Cargo.” *Biological Psychiatry*, Prenatal Programming of Neuropsychiatric Disorders Across the Lifespan, 85, no. 2 (January 15, 2019): 164–71. https://doi.org/10.1016/j.biopsych.2018.09.007.

Nguyen, Minh Q., Zhishang Zhou, Carolyn A. Marks, Nicholas J. P. Ryba, and Leonardo Belluscio. “Prominent Roles for Odorant Receptor Coding Sequences in Allelic Exclusion.” *Cell* 131, no. 5 (November 30, 2007): 1009–17. https://doi.org/10.1016/j.cell.2007.10.050.

Price, Joseph L. “Beyond the Primary Olfactory Cortex: Olfactory-Related Areas in the Neocortex, Thalamus and Hypothalamus.” *Chemical Senses* 10, no. 2 (January 1, 1985): 239–58. https://doi.org/10.1093/chemse/10.2.239.

Price, J. L., and T. P. S. Powell. “The Mitral and Short Axon Cells of the Olfactory Bulb.” *Journal of Cell Science* 7, no. 3 (November 1, 1970): 631–51. https://doi.org/10.1242/jcs.7.3.631.

Rando, Oliver J. “Intergenerational Transfer of Epigenetic Information in Sperm.” *Cold Spring Harbor Perspectives in Medicine* 6, no. 5 (May 1, 2016): a022988. https://doi.org/10.1101/cshperspect.a022988.

Rando, Oliver J., and Kevin J. Verstrepen. “Timescales of Genetic and Epigenetic Inheritance.” *Cell* 128, no. 4 (February 23, 2007): 655–68. https://doi.org/10.1016/j.cell.2007.01.023.

Rechavi, Oded, Leah Houri-Ze’evi, Sarit Anava, Wee Siong Sho Goh, Sze Yen Kerk, Gregory J. Hannon, and Oliver Hobert. “Starvation-Induced Transgenerational Inheritance of Small RNAs in C. Elegans.” *Cell* 158, no. 2 (July 17, 2014): 277–87. https://doi.org/10.1016/j.cell.2014.06.020.

Renier, Nicolas, Eliza L. Adams, Christoph Kirst, Zhuhao Wu, Ricardo Azevedo, Johannes Kohl, Anita E. Autry, et al. “Mapping of Brain Activity by Automated Volume Analysis of Immediate Early Genes.” *Cell* 165, no. 7 (June 16, 2016): 1789–1802. https://doi.org/10.1016/j.cell.2016.05.007.

Ressler, Kerry J., Susan L. Sullivan, and Linda B. Buck. “Information Coding in the Olfactory System: Evidence for a Stereotyped and Highly Organized Epitope Map in the Olfactory Bulb.” *Cell* 79, no. 7 (December 30, 1994): 1245–55. https://doi.org/10.1016/0092-8674(94)90015-9.

Santoro, Stephen W., and Catherine Dulac. “The Activity-Dependent Histone Variant H2BE Modulates the Life Span of Olfactory Neurons.” *ELife* 1 (December 13, 2012): e00070. https://doi.org/10.7554/eLife.00070.

Schmitz, Robert J., Matthew D. Schultz, Mathew G. Lewsey, Ronan C. O'Malley, Mark A. Urich, Ondrej Libiger, Nicholas J. Schork, and Joseph R. Ecker. "Transgenerational Epigenetic Instability Is a Source of Novel Methylation Variants." *Science* 334, no. 6054 (October 21, 2011): 369–73. https://doi.org/10.1126/science.1212959.

Sharma, Upasna, Fengyun Sun, Colin C. Conine, Brian Reichholf, Shweta Kukreja, Veronika A. Herzog, Stefan L. Ameres, and Oliver J. Rando. "Small RNAs Are Trafficked from the Epididymis to Developing Mammalian Sperm." *Developmental Cell* 46, no. 4 (August 20, 2018): 481-494.e6. https://doi.org/10.1016/j.devcel.2018.06.023.

Shykind, Benjamin M., S. Christy Rohani, Sean O'Donnell, Adriana Nemes, Monica Mendelsohn, Yonghua Sun, Richard Axel, and Gilad Barnea. "Gene Switching and the Stability of Odorant Receptor Gene Choice." *Cell* 117, no. 6 (June 11, 2004): 801–15. https://doi.org/10.1016/j.cell.2004.05.015.

Toussaint, Andre B., William Foster, Jessica M. Jones, Samuel Kaufmann, Meghan Wachira, Robert Hughes, Angela R. Bongiovanni, et al. "Chronic Paternal Morphine Exposure Increases Sensitivity to Morphine-Derived Pain Relief in Male Progeny." *Science Advances* 8, no. 7 (February 18, 2022): eabk2425. https://doi.org/10.1126/sciadv.abk2425.

Vassar, Robert, Steve K. Chao, Raquel Sitcheran, Jennifer M. Nuñez, Leslie B. Vosshall, and Richard Axel. "Topographic Organization of Sensory Projections to the Olfactory Bulb." *Cell* 79, no. 6 (December 16, 1994): 981–91. https://doi.org/10.1016/0092-8674(94)90029-9.

Watt, William C., Hitomi Sakano, Zong-Yi Lee, Jane E. Reusch, Kien Trinh, and Daniel R. Storm. "Odorant Stimulation Enhances Survival of Olfactory Sensory Neurons via MAPK and CREB." *Neuron* 41, no. 6 (March 25, 2004): 955–67. https://doi.org/10.1016/s0896-6273(04)00075-3.

Xu, Zhiwei, Avital Adler, Hong Li, Luis M. Pérez-Cuesta, Baoling Lai, Wei Li, and Wen-Biao Gan. "Fear Conditioning and Extinction Induce Opposing Changes in Dendritic Spine Remodeling and Somatic Activity of Layer 5 Pyramidal Neurons in the Mouse Motor Cortex." *Scientific Reports* 9, no. 1 (March 15, 2019): 4619. https://doi.org/10.1038/s41598-019-40549-y.

Yu, Ruby, Xiaoyi Wang, and Danesh Moazed. "Epigenetic Inheritance Mediated by Coupling of RNAi and Histone H3K9 Methylation." *Nature* 558, no. 7711 (June 2018): 615–19. https://doi.org/10.1038/s41586-018-0239-3.